Correspondence to:
A. D. Sproson and D. Selby,
a.d.sproson@durham.ac.uk;
david.selby@durham.ac.uk

Author Contributions:
Formal analysis: Mathieu Dellinger

Tracing the Impact of Coastal Water Geochemistry on the Re-Os Systematics of Macroalgae: Insights From the Basaltic Terrain of Iceland

Adam D. Sproson[1,2] [ID], David Selby[1,3] [ID], Abdelmouchine Gannoun[4], Kevin W. Burton[1], Mathieu Dellinger[5] [ID], and Jeremy M. Lloyd[5] [ID]

[1]Department of Earth Sciences, Durham University, Durham, UK, [2]Atmosphere and Ocean Research Institute, The University of Tokyo, Kashiwa, Japan, [3]State Key Laboratory of Geological Processes and Mineral Resources, School of Earth Resources, China University of Geosciences, Wuhan, China, [4]Laboratoire Magmas et Volcans, Université Clermont Auvergne - CNRS, Campus Universitaire des Cézeaux, Aubière Cedex, France, [5]Department of Geography, Durham University, Durham, UK

Abstract This study presents rhenium (Re) and osmium (Os) elemental and isotope data for macroalgae, dissolved load, and bed load from Icelandic coastal and/or river waters, an environment adjacent to predominantly basaltic terrains, ranging in age from historic to ~12 Ma. Both the Re (0.1 to 88.4 ppb) and Os (3.3 to 254.5 ppt) abundance in macroalgae are shown to be primarily controlled by uptake from the dissolved load of local seawater and are largely dependent on the relative influence of local freshwater inputs. Incorporation of Re and Os into macroalgae appears to be complicated by additional Re and Os uptake from the bed load. The $^{187}Os/^{188}Os$ (0.16 to 0.99) composition of macroalgae is highly variable and is explained in terms of an unradiogenic $^{187}Os/^{188}Os$ contribution from rivers draining younger basaltic catchments that have undergone congruent weathering (and/or hydrothermal input) and a radiogenic $^{187}Os/^{188}Os$ contribution from two distinct sources: rivers draining older catchments that have undergone incongruent weathering of radiogenic primary basaltic minerals and North Atlantic seawater. The $^{187}Re/^{188}Os$ composition (~65 to 40,320) of macroalgae traces that of water, with higher values associated with higher salinity waters, but far exceeds the $^{187}Re/^{188}Os$ of water due to the preferential uptake of Re over Os by macroalgae in areas of high dissolved and/or bed load Re abundances. This study substantiates the utility of macroalgae as a proxy for the long-term (months to years) average $^{187}Os/^{188}Os$ composition of seawater, which holds the potential to elucidate a range of Earth system and anthropogenic processes.

1. Introduction

The Os isotope composition ($^{187}Os/^{188}Os$) of seawater reflects the balance between radiogenic (high $^{187}Os/^{188}Os$) continental-derived and unradiogenic (low $^{187}Os/^{188}Os$) extraterrestrial- and mantle-derived (hydrothermal) sources and has become a powerful tracer of continental weathering, ocean anoxic events, extraterrestrial impacts, and anthropogenic contamination related to the widespread use of PGE ores (e.g., Chen et al., 2009; Peucker-Ehrenbrink & Ravizza, 2000, 2012). In the modern open ocean, the $^{187}Os/^{188}Os$ composition of seawater has been reasonably well constrained through direct analysis using ultralow blank techniques capable of oxidizing all osmium to a common oxidation state (Chen & Sharma, 2009; Gannoun & Burton, 2014; Levasseur et al., 1998; Paul et al., 2009). Nevertheless, direct analysis of seawater remains analytically challenging because of the aforementioned low concentrations and multiple oxidation states (Peucker-Ehrenbrink et al., 2013). There are significant advantages to the use of biomonitors when economic considerations preclude the use of expensive and complex methods for direct seawater measurements and when integrating seasonal or spatial fluctuations (Connan & Stengel, 2011). An ideal biomonitor should be a net accumulator of the element in question with a sufficient mass for analysis, while also being abundant, sedentary, long lived, and available for sampling year-round (Ho, 1990; Rainbow, 1995). Macroalgae (seaweed) fulfill these requirements for a range of metals and have been widely utilized in biomonitoring studies of coastal areas (e.g., Connan & Stengel, 2011; Rönnberg et al., 1990; Viana et al., 2010).

Macroalgae are known to accumulate Re and Os from seawater (Mas et al., 2005; Prouty et al., 2014; Racionero-Gómez et al., 2016; Racionero-Gómez et al., 2017; Rooney et al., 2016; Scadden, 1969; Yang, 1991), and recent studies have shown that macroalgae can act as a proxy for the $^{187}Os/^{188}Os$ of the seawater in which it lived

(Racionero-Gómez et al., 2017) and has been utilized to trace coastal inputs (Rooney et al., 2016). In addition, the ^{187}Re/^{188}Os of macroalgae has provided important insights into the incorporation of Re and Os into organic matter and sedimentary material (Racionero-Gómez et al., 2016; Racionero-Gómez et al., 2017). However, the sources from which Re and Os are taken up, the influence of tidal mixing on the ^{187}Os/^{188}Os and ^{187}Re/^{188}Os of macroalgae and the cause of exceptionally high Re abundance and thus extremely high ^{187}Re/^{188}Os compositions in macroalgae are not fully understood (Mas et al., 2005; Prouty et al., 2014; Racionero-Gómez et al., 2016; Racionero-Gómez et al., 2017; Rooney et al., 2016; Scadden, 1969; Yang, 1991).

This study presents Re-Os abundance and isotope data for macroalgae and dissolved (filtered water) and bed (sediment) loads from coastal waters and rivers draining the basaltic watersheds of Iceland. Iceland consists of an essentially monolithological basaltic terrain of varying ages (historic to 12 Ma) that has resulted in a large range in the ^{187}Os/^{188}Os compositions (0.15 to 1.04), Os abundance (1.01 to 20.5 ppq), and ^{187}Re/^{188}Os values of riverine dissolved loads (Gannoun et al., 2006). Unradiogenic ^{187}Os/^{188}Os values are attributed to congruent basalt weathering and/or hydrothermal input, with radiogenic ^{187}Os/^{188}Os values arising from two distinct processes. The ^{187}Os/^{188}Os compositions of the glacier-fed rivers can be explained by the entrainment of seawater aerosols into precipitation and subsequent glacial melting. Whereas, the ^{187}Os/^{188}Os composition of direct-runoff and spring-fed rivers are explained by the incongruent weathering of certain primary basaltic minerals (olivine, pyroxene, and plagioclase) that possess exceptionally high ^{187}Re/^{188}Os values (288 to 7164), which over time evolves to yield radiogenic ^{187}Os/^{188}Os values (Gannoun et al., 2004).

Iceland therefore provides a unique environment with respect to ^{187}Os/^{188}Os, ^{187}Re/^{188}Os, and Re and Os abundance in which to test the biological and environmental controls on Re-Os uptake and isotope systematics in macroalgae. The results of this study suggest that macroalgae incorporate Re and Os not only from the dissolved load but also from the local bed load. The ^{187}Re/^{188}Os of macroalgae traces that of the water in which it lives. However, exceptionally high ^{187}Re/^{188}Os values in macroalgae may also be caused by selective uptake of Re over Os at high dissolved and/or bed load Re abundances. The results from this study demonstrate the ability of macroalgae to record a time integrated ^{187}Os/^{188}Os composition of the water in which it lived. In addition, the data are also utilized to determine the influence of basaltic weathering on the Re-Os systematics of the North Atlantic seawater.

2. Materials and Methods

2.1. Sampling and Storage

Macroalgae, bed load (sediment), and water from the Icelandic coastline were sampled at 18 locations during late August of 2014 (samples 7–23 and 27). A further nine locations were sampled between late July and early August of 2015 (samples 1–6 and 24–26). In total 27 macroalgae, 11 bed loads, and seven water samples were collected at low tide (Figure 1). Twelve (IS: 2, 4 to 6, 9, 12, 13, 17, 19, 22, 25, and 28) previously collected Icelandic river water samples were also analyzed for Re abundance (see Gannoun et al., 2006 for sample locations). Further information on the sample descriptions, sampling procedures and macroalgae ecology can be found in the supporting information (Carlson, 1991; Gunnarsson & Ingolfsson, 1995; Mathieson et al., 1976; Munda, 1972, 1975, 1987; Niemeck & Mathieson, 1976; Peckol et al., 1988; Sideman & Mathieson, 1983; Strömgren, 1977). Four species of brown macroalgae (*Fucus vesiculosus*, *Fucus spiralis*, *Fucus distichus* and *Ascophyllum nodosum*) were used for analysis. The macroalgae were washed thoroughly using tap water and then deionized (Milli-Q™) water to remove any attached sediment and salt. Subsamples for analysis were then cleaned with tissue to remove any remaining attached particulates and rinsed with MQ again. Likewise, the bed load samples were also thoroughly rinsed with Milli-Q™ to remove any salt water. The samples were then dried for 12 hr at 60 °C and stored in plastic zip-lock bags. Dried macroalgae and bed load samples were crushed/powdered using an agate pestle and mortar prior to analysis. Water samples were filtered through 0.2-μm cellulose acetate filters using a pressurized Sartorius® Teflon unit. Filtrate aliquots were stored in pre-cleaned Savillex® Teflon bottles to prevent Os contamination (Sharma et al., 2012) and are herein referred to as the dissolved load. Salinity was measured using a Hanna® HI 98192 conductivity meter.

2.2. Re-Os Analysis

The Re-Os analyses of macroalgae and bed load were carried out in the Durham Geochemistry Centre (Laboratory for Sulfide and Source Rock Geochronology and Geochemistry and Arthur Holmes Laboratory).
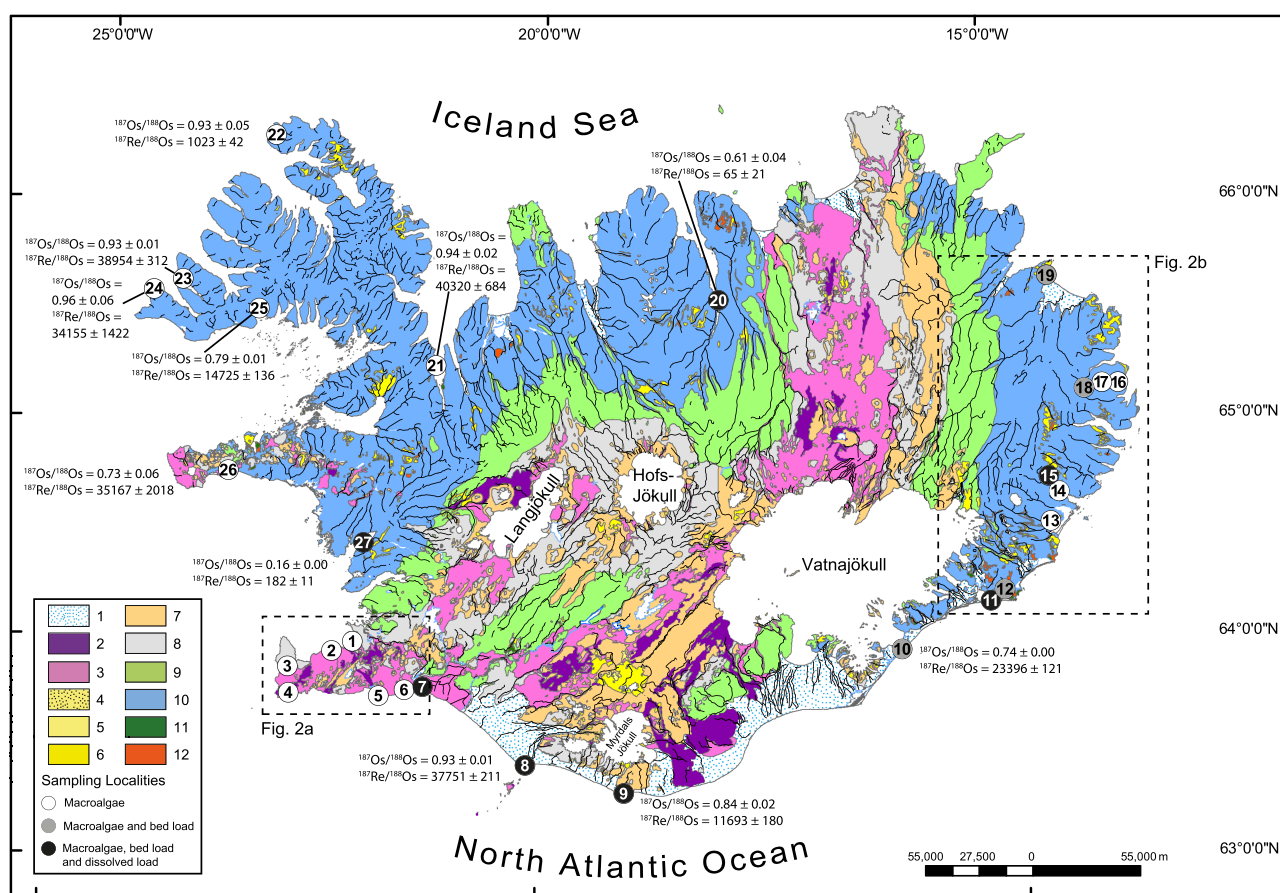
Figure 1. Geological map of Iceland modified after Jóhannesson (2014): 1 = Holocene sediments; 2 = basic and intermediate lavas (postglacial, historic, younger than CE 871); 3 = basic and intermediate lavas (postglacial, prehistoric, older than CE 871); 4 = acid lavas (postglacial, historic, younger than CE 871); 5 = acid lavas (postglacial, prehistoric, older than CE 871); 6 = acid extrusives (Miocene, Pliocene and Pleistocene, older than 11,000 years); 7 = basic and intermediate hyaloclastite, pillow lava and associated sediments (Upper Pleistocene, younger than 0.8 Myr); 8 = basic and intermediate interglacial and supraglacial lavas with intercalated sediments (Upper Pleistocene, younger than 0.8 Myr); 9 = basic and intermediate extrusive rocks with intercalated sediments (Upper Pliocene and Lower Pleistocene, 0.8–3.3 Myr); 10 = basic and intermediate extrusive rocks with intercalated sediments (Miocene and Lower Pliocene, older than 3.3 Myr); 11 = basic and intermediate intrusions, gabbro, dolerite and diorite; 12 = acid intrusions, rhyolite, granophyre, and granite. Sample type and localities are indicated in the legend. The dashed lines represent an outline of areas shown in Figures 2a and 2b.

The seawater Os analyses were conducted at Laboratoire Magmas et Volcans at the Campus Universitaire des Cézeaux, with the Re fraction processed at the Durham Geochemistry Centre.

2.2.1. Macroalgae

The technique for chemical separation of Re and Os from macroalgae is reported by Racionero-Gómez et al. (2017). In brief, approximately 200 mg of powdered macroalgae was introduced into a Carius tube together with 11 N HCl (3 ml), 15.5 N HNO_3 (6 ml), and a known amount of a mixed $^{185}Re + ^{190}Os$ tracer solution and heated to 220 °C in an oven for 24 hr. The Os was isolated from the acid medium using $CHCl_3$ solvent extraction and then back extracted into HBr. The Os was further purified using a CrO_3-H_2SO_4-HBr microdistillation (Birck et al., 1997; Cohen & Waters, 1996). The remaining Re-bearing acid medium was evaporated to dryness at 80 °C, with the Re isolated and purified using both NaOH-acetone solvent extraction and HNO_3-HCl anion chromatography (Cumming et al., 2013).

2.2.2. Bed Load (Sediment)

The detailed analytical procedure of silicates has been adapted from Ishikawa et al. (2014). Approximately 1 g of bed load was crushed using an agate mortar. The powder was dissolved with HCl + HF (4 ml: 2 ml) in a 22-ml savillex® vial at 100 °C. The acid-sample medium was evaporated to dryness at 80 °C before 11 N HCl (1 ml) was added and subsequently evaporated twice to remove remaining HF. The resulting

acid medium was introduced into a Carius tube together with 11 N HCl (3 ml), 15.5 N HNO_3 (6 ml), and a known amount of a mixed ^{185}Re + ^{190}Os tracer solution and heated at 220 °C for 48 hr. The extraction and purification of the Os and Re fractions then followed that described in section 2.2.1.

2.2.3. Dissolved Load (Water)

Filtered Icelandic river samples from Gannoun et al. (2006) were analyzed directly (see section 2.2.4). Filtered Icelandic coastal water samples collected during this study underwent the chemical separation of Re and Os following the technique reported by Racionero-Gómez et al. (2017). Briefly, ~60 g of water samples, plus a known amount of mixed (^{190}Os + ^{185}Re) tracer solution, together with 2 ml of Br_2, 2 ml of CrO_3-H_2SO_4 solution, and 1.5 ml of 98% H_2SO_4, were sealed into a 120 ml savillex vial and heated to 100 °C in an oven for 72 hr to equilibrate sample and spike (Gannoun & Burton, 2014). The Os was extracted from the sample into liquid Br_2 followed by a second extraction of Os using 1 ml of Br_2. The 1 ml of liquid Br_2 was added to the sample solution, reacted for 1 hr, and then removed. The extracted Br_2 is mixed with 1 ml of 9 N HBr and evaporated to dryness and further purified using a CrO_3-H_2SO_4-HBr microdistillation. For the Re purification, 1 ml of the sample-CrO_3-H_2SO_4 solution was evaporated to dryness at 80 °C. The process of Re purification then followed that outlined in section 2.2.1.

2.2.4. Mass Spectrometry

The purified Re and Os fractions were loaded onto Ni and Pt filaments, respectively, and measured using NTIMS (Creaser et al., 1991; Völkening et al., 1991) on a Thermo Scientific TRITON mass spectrometer using Faraday collectors in static mode and an electron multiplier in dynamic mode, respectively. The Re and Os abundances and isotope compositions are presented with 2 SE (standard error) absolute uncertainties, which include full error propagation of uncertainties in the mass spectrometer measurements, blank, spike calibrations, and sample and spike weights. Full analytical blank values for the macroalgae analysis are 10.9 ± 5.9 pg for Re, 0.13 ± 0.13 pg for Os, with a ^{187}Os/^{188}Os composition of 0.61 ± 0.34 (1 SD, $n = 4$). For the bed load analysis, the full analytical blank values are 15.9 ± 0.23 pg for Re, 2.12 ± 0.01 pg for Os, with a ^{187}Os/^{188}Os composition of 0.271 ± 0.001 (2 SE, $n = 1$). For the dissolved load analysis, the full analytical blank values are 10 ± 1.3 pg for Re, 0.043 ± 0.002 pg for Os, with a ^{187}Os/^{188}Os composition of 0.72 ± 0.02 (1 SD, $n = 4$). Analytical blanks were calculated by carrying out the full chemical procedure alongside samples. Bed load and dissolved load samples were corrected using average blank values listed above. Macroalgae sample blanks were more variable and corrected using the individual blank values for each sample run. Blank percentages for macroalgae, bed load, and dissolved load are presented in Tables S1, S2, and S3, respectively.

To monitor the long-term reproducibility of mass spectrometer measurements, Re and Os (DROsS, DTM) reference solutions were analyzed. The 125 pg Re solution yields an average ^{185}Re/^{187}Re ratio of 0.5987 ± 0.0023 (2 SD, $n = 8$), which is in agreement with published values (Cumming et al., 2013, and references therein). A 50 pg DROsS solution gave an ^{187}Os/^{188}Os ratio of 0.16111 ± 0.0008 (2 SD, $n = 8$), which is in agreement with reported value for the DROsS reference solution (Nowell et al., 2008). For the dissolved load Os analysis at the Laboratoire Magmas et Volcans instrument reproducibility was monitored using a 1 pg DTM Os solution, which yields a ^{187}Os/^{188}Os value of 0.1740 ± 0.0002 (2 SD, $n = 4$), which is in agreement with published values (Chen & Sharma, 2009; Gannoun & Burton, 2014).

Direct analysis of dissolved load Re abundance in Icelandic river samples (Gannoun et al., 2006) was measured by quadrupole inductively coupled plasma–mass spectrometry (Q-ICP-MS; Agilent Technologies 7900). A set of seven standards with varying Re abundances and a similar matrix to river water were used for external calibration. Standard and samples were doped with a known concentration of internal standard Tb and Bi to correct for instrumental drift. During the course of the session, standards SLRS-5 and SLRS-6 diluted by a factor 100, and undiluted, were measured several times. The mean measured values for both standards are as follows: SLRS-5 diluted 100 times is 0.57 ± 0.05 ppt (2 SE, $n = 8$), SLRS-6 diluted 100 times is 0.12 ± 0.01 ppt (2 SE, $n = 2$), undiluted SLRS-5 is 58.9 ppt ($n = 1$), and undiluted SLRS-6 is 13.1 ppt ($n = 1$). The measured values for SLRS-5 are in good agreement with published values (Horan et al., 2017; Yeghicheyan et al., 2013). The long-term reproducibility of the Re concentration measurements is better than ± 8%. Rhenium abundance data from Icelandic rivers have been compiled with Os abundance measurements from Gannoun et al. (2006) in Table S4. The ^{187}Re/^{188}Os of Icelandic riverine samples was estimated from measured total Re and Os abundances using the average composition of ^{187}Re (62.6%) and ^{188}Os (13.2%) in natural samples (Table S4).

3. Results

3.1. Macroalgae

The Re and Os abundance and isotope data for macroalgae are presented in Table S1. Rhenium and Os abundances show a large range from 0.1 to 88.4 ppb and from 3.3 to 254.5 ppt, respectively. Individual species, such as *Fucus vesiculosus*, *Fucus spiralis*, *Fucus distichus*, and *Ascophyllum nodosum*, show variable Re abundances from 3.6 to 71.9 ppb, 14.5 to 28.8 ppb, 0.1 to 1.6 ppb, and 3.2 to 88.4 ppb, respectively (Figure 3a). The same individual species show a large range in Os abundances from 5.0 to 254.5 ppt, 3.3 to 14.5 ppt, 4.7 to 7.6 ppt, and 9.5 to 53 ppt, respectively (Figure 3a). The ^{187}Os/^{188}Os compositions of the macroalgae range from 0.16 to 0.99 (Figure 3b). The ^{187}Re/^{188}Os ratios of the macroalgae are also highly variable, ranging from 65 to 40,320 (Figure 3b).

Rhenium and Os abundance in macroalgae are consistent with previous studies, showing a large range in values (Figure 3a). Rhenium abundances in *Fucus vesiculosus* from sample location 3, 8, 10, and 24 (Figure 1) compare well with values of 51 to 103.4 ppb in the UK (Racionero-Gómez et al., 2016) and 60.8 to 84.9 ppb in Norway (Mas et al., 2005). However, most *Fucus vesiculosus* in this study have lower concentrations than those from the literature, ranging from 3.6 to 50.4 ppb. Likewise, *Fucus disichus* and *Ascophyllum nodosum* show a lower abundance of Re than recorded values for California (Yang, 1991) and Greenland (Rooney et al., 2016), with the exception of sample 21. Previous Os abundance determinations for *Fucus vesiculosus* from the UK (33.8 ppt; Racionero-Gómez et al., 2017) and *Ascophyllum nodosum* from Greenland (12.6 ppt; Rooney et al., 2016) fall within the ranges found in this study. However, Os abundance for *Fucus distichus* recorded in Greenland (14 ppt; Rooney et al., 2016) is far higher than the range for Icelandic *Fucus distichus* of this study.

A one-way analysis of variance (ANOVA) test was conducted to determine the effect of macroalgae species on Re and Os abundance and ^{187}Re/^{188}Os and ^{187}Os/^{188}Os compositions. When comparing *Fucus vesiculosus*, *Fucus spiralis*, *Fucus distichus*, and *Ascophyllum nodosum*, the ANOVA tests for Re abundance (F (3, 23) = 2.29; p-value = 0.11), Os abundance (F (3, 23) = 0.45; p-value = 0.72), ^{187}Re/^{188}Os (F (3, 23) = 1.18; p-value = 0.34), and ^{187}Os/^{188}Os (F (3, 23) = 0.68; p-value = 0.57) all have p-values, which fall above the significance level (p-value = 0.05), suggesting that the macroalgae species does not have a significant influence on any parameter considered in this study.

3.2. Bed Load (Sediment)

The Re and Os abundance and isotopic data of the bed load samples are presented in Table S2. Rhenium and Os abundances range from 0.5 to 1.1 ppb and 5.3 to 67.1 ppt, respectively. This compares well with Re and Os abundances previously recorded in Icelandic basalts and riverine bed loads, which range from 0.05 to 1.8 ppb and 3.7 to 1954.9 ppt, respectively (Debaille et al., 2009; Gannoun et al., 2006). Where the bed load Os abundance is <30 ppt, the Os abundance of macroalgae remains consistent at ~10 ppt but increases exponentially where bed load Os abundances are >40 ppt (R^2 = 0.88, p-value = 0.00002; Figure 4a). Macroalgae is enriched in Re by several orders of magnitude when compared to the bed load. A significant linear correlation (R^2 = 0.61, p-value = 0.005) in Re abundance is observed between macroalgae and the corresponding bed load (Figure 4b).

The ^{187}Os/^{188}Os composition of the bed load ranges from 0.15 to 0.71, with an average of 0.28, which is closer to the unradiogenic end-member, similar to previously recorded Icelandic riverine bed loads (Gannoun et al., 2006). In almost all cases, the ^{187}Os/^{188}Os ratios of macroalgae are significantly more radiogenic than the corresponding bed load (Figure 5a). The ^{187}Re/^{188}Os ratio of the bed load ranges from 45 to 879, which fall close to the lower end of the range reported for Icelandic riverine bed loads (45–1698; Gannoun et al., 2006). Although the macroalgae possess much greater ^{187}Re/^{188}Os than the corresponding bed load, a strong linear correlation (R^2 = 0.83, p-value = 0.0001) between the macroalgae and bed load ^{187}Re/^{188}Os is observed (Figure 5b).

3.3. Dissolved Load (Water)

The Re and Os abundance and isotope data of filtered water samples are reported in Table S3. Rhenium and Os abundances range from 0.6 to 10 ppt and 8.1 to 69.2 ppq, respectively. These values are highly variable when compared to oceanic Re (~8.2 ppt; Anbar et al., 1992; Colodner et al., 1993b; Colodner et al., 1995)
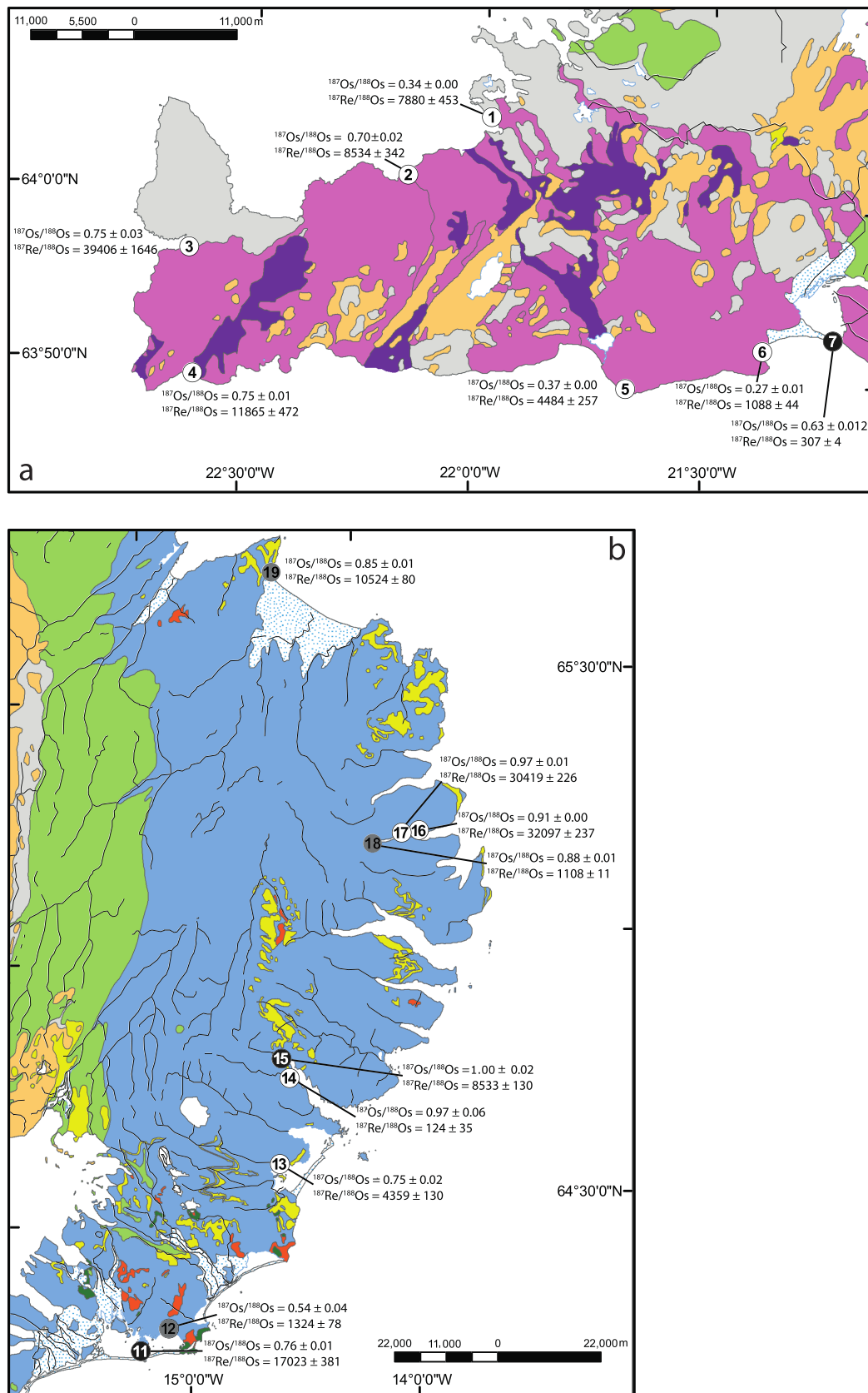
Figure 2. Geological maps of the (a) Reykjanes Peninsula and (b) Eastern Fjords modified after Jóhannesson (2014). Key is the same as in Figure 1.

and Os (~10 ppq; Gannoun & Burton, 2014; Levasseur et al., 1998; Sharma et al., 1997; Woodhouse et al., 1999) concentrations. However, they compare well with Re and Os concentrations found in global river estimates, which range from 24 to 2.3 ppb and 4.6 to 52.1 ppq, respectively (Colodner et al., 1993a; Levasseur et al., 1999; Miller et al., 2011; Sharma & Wasserburg, 1997). The Os concentrations are similar to those previously recorded for Icelandic rivers (1 to 20.5 ppq; Gannoun et al., 2006). The Re concentrations greatly exceed those recorded for Icelandic rivers measured in this study (0.06 to 1 ppt; Table S4). Macroalgae are enriched in Re and Os by several orders of magnitude when compared to the dissolved load of the rivers measured here (Figures 4c and 4d). Macroalgae Os abundance shows no relationship with the Os abundance of the dissolved load (Figure 4c). Macroalgae Re abundance shows a positive correlation with dissolved Re abundance ($R^2 = 0.65$, p-value = 0.03; Figure 4d).

The $^{187}Os/^{188}Os$ ratio of the dissolved load ranges from 0.16 to 0.88, falling within the range of the composition of previously analyzed Icelandic rivers (0.15 to 1.04; Gannoun et al., 2006). The $^{187}Re/^{188}Os$ ratio of the dissolved load ranges from 131 to 5467, exceeding the range of Icelandic rivers (122 to 1659; Table S4). The lower and upper values of this range are similar to average global riverine (227) and seawater (4270) $^{187}Re/^{188}Os$ ratios, respectively (Peucker-Ehrenbrink & Ravizza, 2000), suggesting the influence of both river water and seawater at these sampling locations.

In almost all cases the $^{187}Os/^{188}Os$ ratios of macroalgae are significantly more radiogenic than the corresponding dissolved load (Figure 5c). The most radiogenic values were obtained for macroalgae close to the oldest basalt in the eastern and north-western parts of Iceland, with the most unradiogenic isotope ratios being associated either close to the central active zone or the rivers draining it (Figures 1 and 2). The macroalgae $^{187}Re/^{188}Os$ are generally several times greater than the corresponding dissolved load (Figure 5d). A strong correlation ($R^2 = 0.97$, p-value = 0.00005) in $^{187}Re/^{188}Os$ values is observed between macroalgae and the dissolved load (Figure 5d).

4. Discussion

4.1. Influence of Estuarine Conditions on the Re-Os Systematics of Macroalgae

Macroalgae cultured in a medium possessing artificially varied abundances of Re and Os has been shown to experience an increase in the uptake of both Re (Racionero-Gómez et al., 2016) and Os (Racionero-Gómez et al., 2017) in macroalgae. It has also been shown that the $^{187}Os/^{188}Os$ values of floating macroalgae (*Sargassum fluitans* and *S. natans*) from the Gulf of Mexico (Rooney et al., 2016) are indistinguishable from that of the present-day oceanic $^{187}Os/^{188}Os$ value of 1.06 (Peucker-Ehrenbrink & Ravizza, 2000). In contrast, macroalgae from waters off the west coast of Greenland deviate from this value (0.9–1.9), instead recording the $^{187}Os/^{188}Os$ composition of the local Os flux from the continents into the coastal region (Rooney et al., 2016). This ability of macroalgae to record the local environment $^{187}Os/^{188}Os$ composition has also been shown by *Fucus vesiculosus* from an estuary on the east coast of the UK that records the $^{187}Os/^{188}Os$ of the seawater in which it lives (0.94) and when cultured in seawater doped with Os of a known $^{187}Os/^{188}Os$ composition (0.16), takes on the composition of the new source (Racionero-Gómez et al., 2017). It is therefore postulated that the $^{187}Os/^{188}Os$ of macroalgae can act as a proxy for the Re abundance, Os abundance, $^{187}Os/^{188}Os$, and $^{187}Re/^{188}Os$ of the seawater in which it lives. As such, we therefore expect Re-Os isotope systematics of macroalgae living in an estuarine habitat to be defined by a mixture between local riverine and seawater end-members.

4.1.1. Influence of Estuarine Conditions on the Re and Os Abundance of Macroalgae

Oceanic Re (8.2 ppt) and Os (~10 ppq) concentration are seen to be relatively constant (Anbar et al., 1992; Colodner et al., 1993a; Levasseur et al., 1998; Sharma et al., 1997; Woodhouse et al., 1999) when compared to riverine Re (3.1 ppt) and Os (9.1 ppq) abundance, which is generally much lower, but also highly variable (Colodner et al., 1993a; Levasseur et al., 1999; Miller et al., 2011; Sharma & Wasserburg, 1997). During mixing between these sources in an estuarine habitat, it has been shown that Re behaves conservatively in the Amazon estuary with low concentrations (0.21 ppt) at low salinity and high concentrations (8.6 ppt) at high salinity (Colodner et al., 1993a). This notion is supported by the dissolved load Re abundances from this study (Table S3), which show increasing Re concentration with increasing salinity ($R^2 = 0.83$, p-value = 0.002) from ~2.1 ppt at low salinities to ~10.6 ppt at high salinities. Osmium, on the other hand, has been shown to behave nonconservatively in estuaries, with removal from the water column at low salinities in temperate
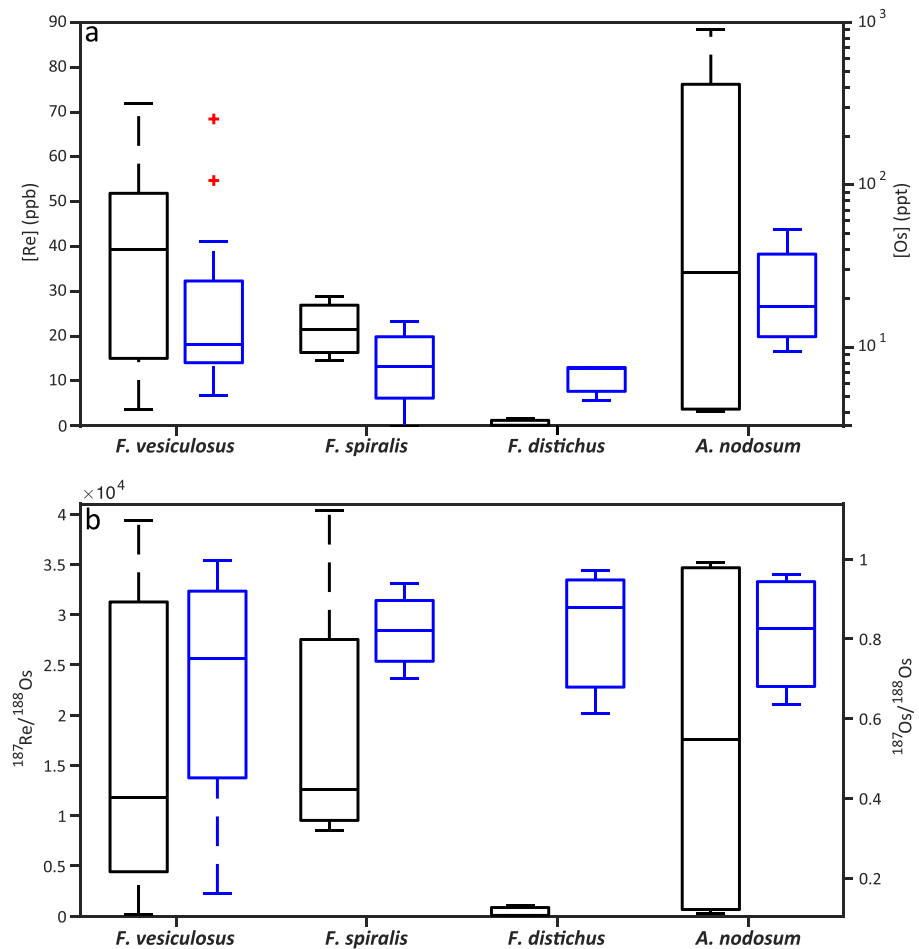
Figure 3. (a) Rhenium (black) and osmium (blue) abundance and (b) ^{187}Re/^{188}Os (black) and ^{187}Os/^{188}Os (blue) isotopic composition boxplots for *F. vesiculosus*, *F. spiralis*, *F. distichus* and *A. nodosum*.

and arctic estuaries (Levasseur et al., 2000; Turekian et al., 2007) and at high salinities in tropical estuaries (Martin et al., 2001; Sharma et al., 2007). The Os abundance of the dissolved load of water measured in this study (8.1 to 69.2 ppq) compares well with global river estimates (4.6–52.1 ppq; Levasseur et al., 1999; Sharma & Wasserburg, 1997). However, with the exception of samples from location 7 and 27, the dissolved load Os abundance shows a relatively small range, with consistently low values at low salinities (8.3 ± 0.3 ppq) and high salinities (13.3 ± 5 ppq).

Much like the dissolved load Re abundances studied here, macroalgae show an increase in Re abundance with salinity, with macroalgae living in low-salinity waters possessing lower Re abundances (~6.9 ppb) than macroalgae living in more saline waters (~35.5 ppb; R^2 = 0.53, p-value = 0.06). In keeping with previous culturing studies (Racionero-Gómez et al., 2016), these data support the notion that macroalgae take up Re from the dissolved load of the water in which they live leading to higher Re abundances in macroalgae at higher dissolved load abundances (Figure 4d; R^2 = 0.65; p-value = 0.03). This may explain some of the interspecies variation in Os and Re abundance (Figure 3a), whereby species living lower in the eulittoral zone, that is, *F. vesiculosus*, generally have a higher abundance than species living higher in the eulittoral zone, that is, *F. spiralis* and *F. distichus* (see Text S2). Much like the dissolved load Os abundances, with the exception of samples from location 7 and 27, macroalgae have relatively consistent Os abundances at low salinities (8.4 ± 1.2 ppt) and high salinities (8.3 ± 1.7 ppt). The lack of variability in the Os abundances found in the dissolved load of water samples studied here may explain the absence of any correlation between the dissolved load and macroalgae in this study (Figure 4c), whereby samples are clustered around a single value (see inset in Figure 4c).
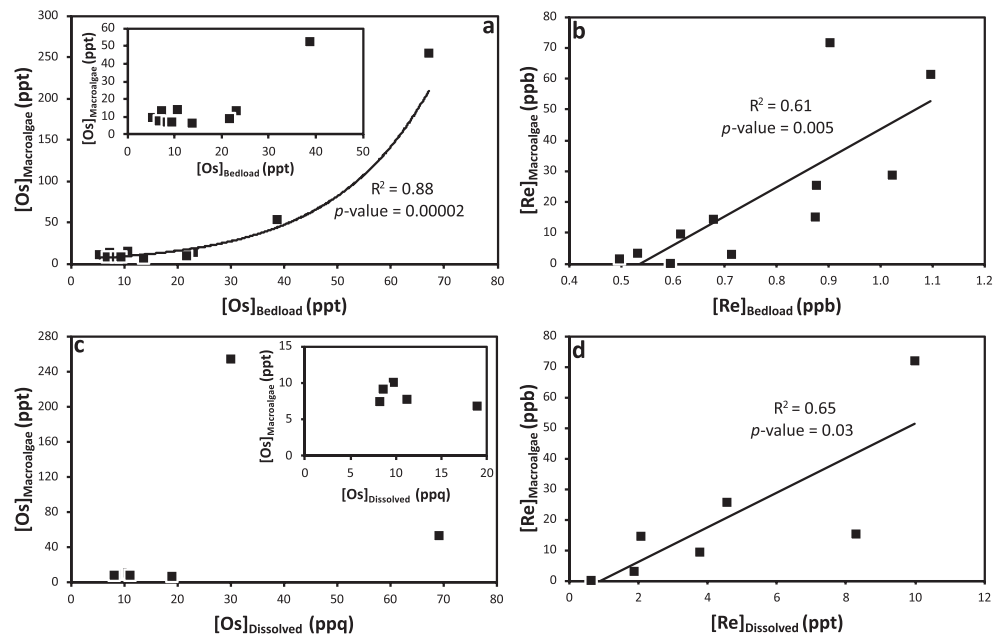
Figure 4. Bed load (a) osmium and (b) rhenium abundance and dissolved load (c) osmium and (d) rhenium abundance versus the corresponding abundance in macroalgae. See text for discussion.

4.1.2. Influence of Estuarine Conditions on ^{187}Re/^{188}Os Composition of Macroalgae

The ^{187}Re/^{188}Os of the dissolved load from this study (131 to 5467) shows a similar range to global (227 to 4270) and Icelandic (275 to 4199) river and seawater estimates (Table S4; Colodner et al., 1993a; Gannoun et al., 2006; Gannoun & Burton, 2014; Peucker-Ehrenbrink & Ravizza, 2000). When the ^{187}Re/^{188}Os of the dissolved load is shown against salinity (blue circles in Figure 6b) we see low ^{187}Re/^{188}Os ratios (131 to 1,184), similar to Icelandic riverine values (122 to 1,659; Table S4; Gannoun et al., 2006), at low salinity (Figure 6b). The ^{187}Re/^{188}Os of the dissolved load remains relatively low (613) until intermediate salinities, where it begins
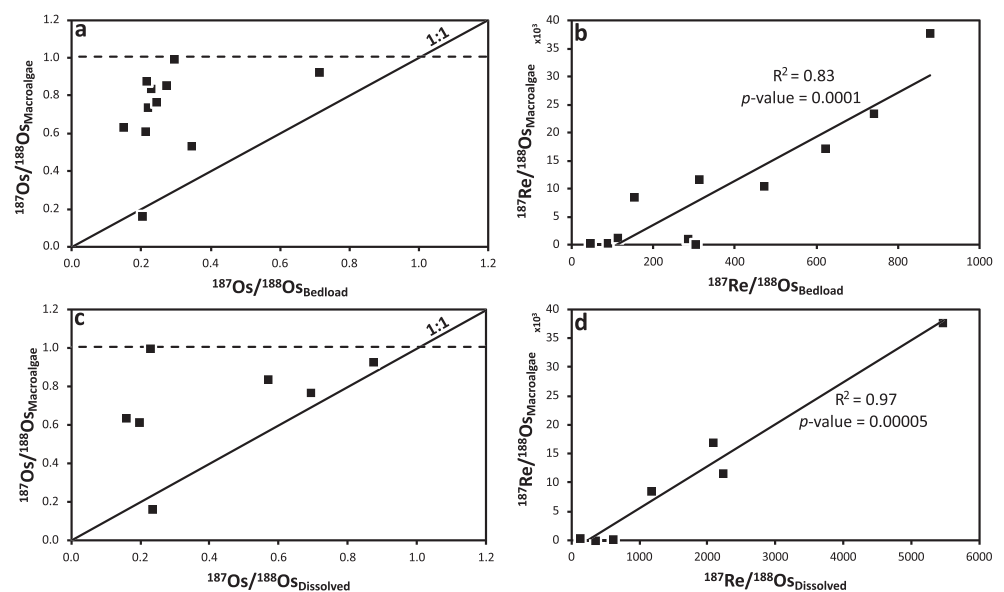

Figure 5. Bed load (a) ^{187}Os/^{188}Os and (b) ^{187}Re/^{188}Os and dissolved load (c) ^{187}Os/^{188}Os and (d) ^{187}Re/^{188}Os versus the corresponding ratio in macroalgae. The dashed line in a and c represents the ^{187}Os/^{188}Os of North Atlantic seawater (Gannoun & Burton, 2014). See text for discussion.
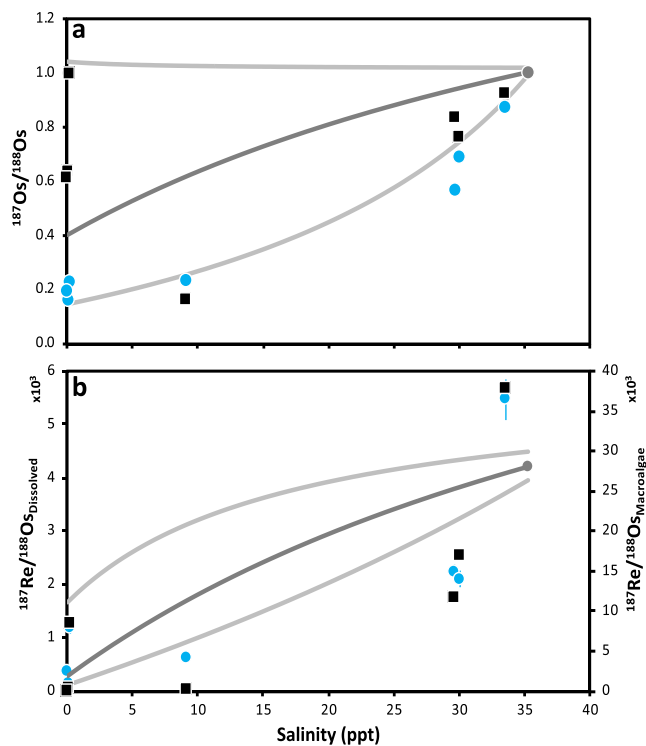
Figure 6. (a) $^{187}Os/^{188}Os$ and (b) $^{187}Re/^{188}Os$ isotopic composition versus salinity. The blue circles, grey circles, and black squares represent dissolved load (this study), North Atlantic seawater (Colodner et al., 1993b; Gannoun & Burton, 2014), and macroalgae (this study), respectively. The grey lines represent idealized mixing between Icelandic river water and North Atlantic seawater. The dark grey line represents mixing between average riverine ($^{187}Os/^{188}Os$ = 0.4, [Os] = 5.7 ppq, and $^{187}Re/^{188}Os$ = 275) and seawater ($^{187}Os/^{188}Os$ = 1.005, [Os] = 9.2 ppq, and $^{187}Re/^{188}Os$ = 4199) values. The upper and lower light grey lines represent mixing between maximum riverine ($^{187}Os/^{188}Os$ = 1.041, [Os] = 1.6 ppq, and $^{187}Re/^{188}Os$ = 1659) and seawater ($^{187}Os/^{188}Os$ = 1.018, [Os] = 9.7 ppq, and $^{187}Re/^{188}Os$ = 4484) isotopic compositions and minimum riverine ($^{187}Os/^{188}Os$ = 0.148, [Os] = 20.5 ppq, and $^{187}Re/^{188}Os$ = 122) and seawater ($^{187}Os/^{188}Os$ = 0.992, [Os] = 8.7 ppq, and $^{187}Re/^{188}Os$ = 3941) isotopic compositions, respectively (Table S4; Colodner et al., 1993b; Gannoun et al., 2006; Gannoun & Burton, 2014). See text for discussion.

to increase toward $^{187}Re/^{188}Os$ values indicative of seawater (grey circle in Figure 6b) at high salinity. The $^{187}Re/^{188}Os$ of the dissolved load from this study falls outside an idealized mixing model based on literature data (grey lines in Figure 6b) at high salinity. This is likely due to the assumed constant mixing between seawater and freshwater sources in the model. Although the Re abundance shows an increase with salinity toward seawater values, Os abundance shows higher values than seawater at high salinity. This will act to drive the $^{187}Re/^{188}Os$ of the dissolved load to lower values than the mixing model (Figure 6b). One dissolved load sample at high salinity (33.6 ppt), on the other hand, is defined by a higher Re abundance, and a similar Os abundance, to that of seawater, which will cause the $^{187}Re/^{188}Os$ of the dissolved load to exceed the upper limits of the mixing model (Figure 6b). These discrepancies can be attributed to the nonconservative nature of Os in Arctic estuaries versus the conservative nature of Re in estuaries, as previously discussed.

The $^{187}Re/^{188}Os$ ratios of macroalgae show a wide range from ~65 to 40,320 (Figure 3b) similar to previous studies (7 to 31,983; Rooney et al., 2016, Racionero-Gómez et al., 2017), but far exceeding the dissolved load of waters measured here (131 to 5467). Despite far higher ratios, the $^{187}Re/^{188}Os$ of macroalgae shows a strong correlation (R^2 = 0.97, p-value = 0.00005) with the $^{187}Re/^{188}Os$ of the dissolved load (Figure 5d). Moreover, when the $^{187}Re/^{188}Os$ of macroalgae is plotted against salinity (black squares in Figure 6b) we see a very similar relationship to the $^{187}Re/^{188}Os$ of the dissolved load (blue circles in Figure 6b). This suggests that the $^{187}Re/^{188}Os$ of the water in which macroalgae resides exerts a strong influence on the $^{187}Re/^{188}Os$ of the macroalgae, with higher values ($>10^4$) reflecting a stronger marine influence, and lower values ($<10^4$) reflecting a stronger freshwater influence (Figure 6b). It is therefore possible to utilize the $^{187}Re/^{188}Os$ of macroalgae as an indicator of the degree of freshwater influence in a marine habitat.

Despite the strong relationship between the $^{187}Re/^{188}Os$ of macroalgae and the $^{187}Re/^{188}Os$ of the dissolved load (Figure 5d), macroalgae still attain $^{187}Re/^{188}Os$ ratios several orders of magnitude greater than the corresponding dissolved load. It has been proposed that macroalgae incorporate Re and Os through the same mechanism leading to competition between these elements and therefore lower Re concentration in macroalgae under higher Os seawater concentration and vice versa (Racionero-Gómez et al., 2017). As previously discussed, higher Re abundance in the dissolved load and therefore macroalgae at high salinities coupled with very little or no change in Os abundance with salinity will lead to higher Re availability at high salinities. This would lead to the preferential uptake of Re over Os in macroalgae at high salinities, leading to exceptionally high $^{187}Re/^{188}Os$ when compared to the $^{187}Re/^{188}Os$ of the surrounding environment.

4.1.3. Influence of Estuarine Conditions on $^{187}Os/^{188}Os$ Composition of Macroalgae

The $^{187}Os/^{188}Os$ of macroalgae from this study (0.16 to 0.88) shows a similar range to the $^{187}Os/^{188}Os$ of dissolved Os in Icelandic rivers (0.15 to 1.04; Gannoun et al., 2006). When the dissolved load from this study is plotted against salinity (blue circles in Figure 6a), the $^{187}Os/^{188}Os$ values at low salinity are close to that expected for highly unradiogenic Icelandic riverine values ($^{187}Os/^{188}Os$ = 0.15; Gannoun et al., 2006). The $^{187}Os/^{188}Os$ of the dissolved load remains relatively unradiogenic (0.24) until intermediate salinities, after which it begins to increase toward the $^{187}Os/^{188}Os$ of North Atlantic surface waters ($^{187}Os/^{188}Os$ = 1.005; grey circle in Figure 6a; Gannoun & Burton, 2014) at high salinity, following the idealized mixing model between minimum riverine and seawater isotopic compositions (lower grey line in Figure 6a) indicative of a strong influence from rivers draining juvenile basaltic catchments at the water collection sites studied here (See

section 4.3 for more details). This overall trend is supported by arctic, temperate, and tropical estuaries, which show an increasing seawater $^{187}Os/^{188}Os$ influence with higher salinities (Levasseur et al., 2000; Martin et al., 2001; Sharma et al., 2007; Turekian et al., 2007).

The $^{187}Os/^{188}Os$ of macroalgae from this study (0.16 to 0.99; Figure 3b) shows a similar range to the $^{187}Os/^{188}Os$ of dissolved load of Icelandic rivers (0.15 to 1.04; Gannoun et al., 2006) and waters studied here (0.16 to 0.88). However, when the $^{187}Os/^{188}Os$ of macroalgae is compared with that of the dissolved load from the same location there is no apparent relationship (Figure 5c). This could be due to the entrainment of seawater in the estuarine habitat from which these macroalgae and water samples were taken. As all water samples in this study were collected at low tide, their values will represent the lowest salinity end-member at their respective geographical locations at the time of collection. Macroalgae (black squares in Figure 6a), on the other hand, were collected from above the low water mark and subsequently will reside in waters that experience a mixing between low tide values (lower grey line in Figure 6a) and more radiogenic seawater values (grey circle in Figure 6a; dashed line in Figure 5c) through a tidal cycle. The composition of macroalgae will therefore represent a mixing between the $^{187}Os/^{188}Os$ of a local freshwater source and the $^{187}Os/^{188}Os$ of North Atlantic seawater (1.02; Gannoun & Burton, 2014).

River mouths reflect mixing between waters from an entire drainage basin, which, in the case of Iceland, have highly variable $^{187}Os/^{188}Os$ (0.15 to 1.04) and $^{187}Re/^{188}Os$ (122 to 1659) compositions (Table S4; Gannoun et al., 2006). Macroalgae samples from low-salinity waters show a large range in both $^{187}Os/^{188}Os$ (Figure 6a) and $^{187}Re/^{188}Os$ (Figure 6b) compositions, falling between the maximum (upper grey line in Figure 6) and minimum (lower grey line in Figure 6) Icelandic riverine estimates (Table S4; Gannoun et al., 2006) suggesting the isotopic composition of macroalgae inhabiting low-salinity waters may reflect changes in the dominant composition of the local drainage basin. Therefore, the $^{187}Os/^{188}Os$ of macroalgae in an estuary represents a long-term average for the $^{187}Os/^{188}Os$ of the dissolved load at that location, reflecting both an integrated freshwater composition and the degree to which this freshwater source dominates relative to seawater.

Although spatially integrated measurements for an entire drainage region can be achieved by sampling at the river mouth, intrariver variability means only time series measurements, flux-weighted to give a yearly average, are truly reliable (Miller et al., 2011 and references therein). The difficulty in obtaining river samples for specific locations and times can lead to temporal biasing, with many river systems overestimated or underestimated with respect to flux and/or isotopic composition (Miller et al., 2011). This study suggests that macroalgae measurements could potentially overcome some of the problems associated with temporal biasing. As macroalgae take up Re and Os throughout their life, with no evidence of subsequent release (Racionero-Gómez et al., 2016, 2017), their Re and Os abundance and isotopic composition will represent a time-averaged value, which can be used to determine the flux and isotopic composition of the waters they inhabit.

It has been shown that the levels of other metals in macroalgae may vary with salinity, temperature, season, growth rate, position in the intertidal zone, or age (Barreiro et al., 2002; Bryan & Hummerstone, 1973; Burdon-Jones et al., 1982; Connan & Stengel, 2011; Fuge & James, 1973; Rice & Lapointe, 1981), which are highly variable in Iceland (See Text S2). As such, individual macroalgae Re and Os abundance and isotopic composition may become biased to the water signatures present at times of more favorable uptake and/or growth conditions. More work is needed to be done to determine the specific response of Re and Os uptake to these environmental parameters.

4.2. Influence of the Bed Load on the Re-Os Systematics of Macroalgae

Although the relationship between the dissolved load and macroalgae is evident from the literature, previous studies have not looked into Re and Os uptake in macroalgae from the bed load. A strong correlation between the bed load Re and Os abundance and Re ($R^2 = 0.61$, p-value = 0.005) and Os ($R^2 = 0.88$, p-value =- 0.00002) abundance in macroalgae (Figures 4a and 4b) suggests a potential additional source of Re and Os to macroalgae from the bed load. In the case of Os, this additional source from the bed load seems to have little influence on the Os abundance of macroalgae, which remains at ~10 ppt, at low bed load concentrations (<30 ppt) (see inset in Figure 4a). At high concentrations (>30 ppt), this additional source could have a strong

influence on the macroalgae Os abundance (Figure 4a). However, this observation is only shown by two samples from location 7 and 27.

The additional uptake of Re from the bed load (Figure 4b) coupled to no Os uptake from the bed load at low (<25 ppt) Os bed load concentrations (Figure 4a) may lead to an increase in macroalgae Re abundance in environments with greater Re bed load abundances. As previously discussed for the dissolved load, this additional source in Re could lead to an increase in the $^{187}Re/^{188}Os$ of macroalgae to values far greater than any known Icelandic geochemical reservoir and a positive correlation with the $^{187}Re/^{188}Os$ of the underlying bed load (Figure 5b; $R^2 = 0.83$, p-value $= 0.0001$).

The holdfast serves as an anchor to the underlying substrate and does not act as the primary organ for nutrient and water uptake as evidenced by consistently low Re and Os abundance of the holdfast in *F. vesiculosus* when compared to the other parts of the organism (Racionero-Gómez et al., 2016, 2017). It is more likely that macroalgae will come into contact with the bed load during exposure at low tides. Moreover, despite not being measured in this study, it has been shown that Re and Os abundance in the suspended particulate load, recovered from the acetate filters (0.2 μm) of Icelandic river water samples, positively correlates with the respective bed load (Gannoun et al., 2006). The similarity of the bed load Re (0.5 to 1.1 ppb) and Os (5.3 to 67.1 ppt) abundance measured in this study to Icelandic river Re (0.3–1.8 ppb) and Os (4.2 to 34.9 ppt) bed load abundances (Gannoun et al., 2006) could suggest a correlation with Re and Os in the suspended particulate load at the sampled locations, and macroalgae could therefore come into contact with underlying sediment during resuspension of the bed load. The macroalgae Re and Os abundance could therefore potentially be correlated with the suspended particulate load; however, the particulate load was not measured in this study, so we can only comment.

Additional uptake of heavy metals by macroalgae from the bed load has received considerable attention in the literature. Contamination from adhering particles such as bacteria, microalgae, or fine sediment accounts for a considerable proportion of Cr, Fe, Al, and Pb in aquatic plants, including macroalgae (Barreiro et al., 2002, and references therein). Higher levels of adhered particles could therefore lead to greater abundances of Re and Os in macroalgae. Moreover, it has previously been suggested that the selectivity coefficient between macroalgae polyphenolic proteins and metals such as Cu, Zn, Cd, As, Pb, Ag, and Cr exceeds the binding strength of these metals with sediment particles, allowing macroalgae to scavenge these metals directly from particulates (Barreiro et al., 2002; Haritonidis & Malea, 1999; Luoma et al., 1982; Malea et al., 1995; Ragan et al., 1979).

It has also been suggested that Re is not associated with the cell wall, intercellular matrix, chloroplasts, or cytoplasmic proteins suggesting a different uptake pathway from the particulates (Racionero-Gómez et al., 2016; Xiong et al., 2013; Yang, 1991). Instead, the alginate and fucoidan matrix shows a strong affinity for Re suggesting possible storage in macroalgae cellular membrane proteins (Xiong et al., 2013). Rhenium is often associated with protonated amino groups suggesting these amino groups participate in the absorption of Re into macroalgae (Melián et al., 2000; Xiong et al., 2013). If the affinity for amino groups is greater than the binding strength with sediment, it would allow Re to be scavenged from the sediment. Moreover, it has been suggested that macroalgae have similar binding sites and uptake pathways for Re and Os (Racionero-Gómez et al., 2017), suggesting that Os could be taken up from sediment particles in a similar manner to Re.

When trying to determine the contribution of Re and Os to macroalgae from the dissolved load, the Re and Os abundances in macroalgae could become highly biased by regions with high bed load Re and Os abundances. Previous work has utilized the macroalgae/sediment ratio for Al (Barreiro et al., 2002) and Fe (Luoma et al., 1982) to determine the maximum potential contribution from particulate metals to macroalgae. This value can then be utilized to correct metal abundances to determine the contribution from the dissolved load more accurately (Barreiro et al., 2002; Luoma et al., 1982). Future work will need to utilize Al and/or Fe abundances in sediments and macroalgae to correct for Re and Os uptake from local sediments.

4.3. Influence of Basaltic Weathering on the $^{187}Os/^{188}Os$ and $^{187}Re/^{188}Os$ of Macroalgae

During mantle melting and basalt genesis, both Re and Os become fractionated. Osmium behaves as a compatible element during melting and is retained in the mantle, unlike Re, which is moderately incompatible and enters the melt. Mantle derived basalts thus have very high Re/Os values and their primary mineral phases crystallize in a high Re/Os environment (Burton et al., 2002; Gannoun et al., 2004). Primary minerals
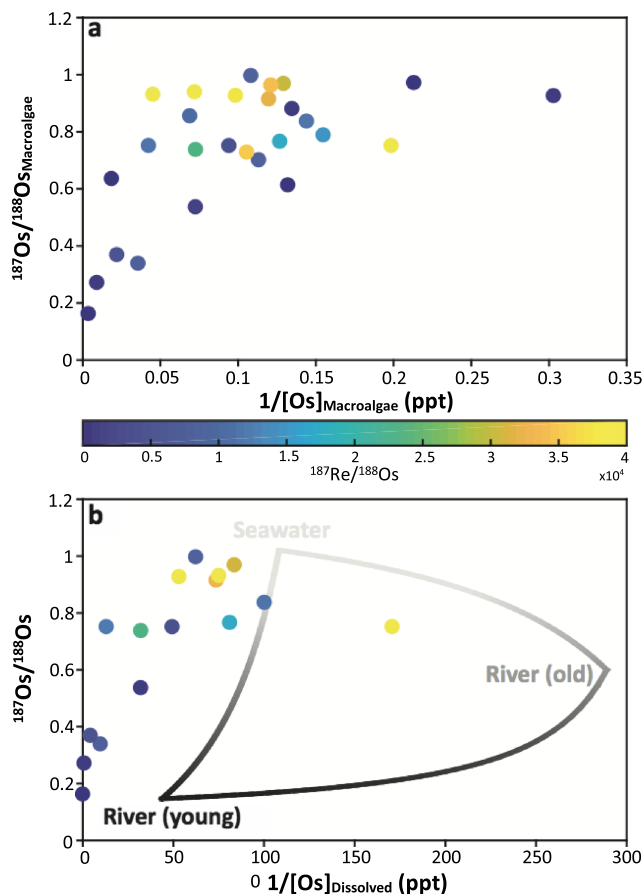
Figure 7. Osmium isotopic (^{187}Os/^{188}Os) composition against the reciprocal of the Os abundance for (a) macroalgae and (b) *F. vesiculosus*. In b, the Os abundance has been converted to that of seawater using the relationship found in Racionero-Gómez et al. (2017). The three-point end-member mixing diagram is based on extreme North Atlantic seawater (light grey; Gannoun & Burton, 2014) and rivers draining a young basaltic catchment (black; Gannoun et al., 2006) and old basaltic catchment (dark grey, Gannoun et al., 2006). The color of the symbol denotes the ^{187}Re/^{188}Os of macroalgae. See text for discussion.

such as olivine, pyroxene, and plagioclase possess higher ^{187}Re/^{188}Os than bulk-rock or glass, and over relatively short timescales ($<10^6$ years) can produce measurable shifts in ^{187}Os/^{188}Os through ingrowth of radiogenic osmium (^{187}Os^r; see Figure 9 in Gannoun et al., 2006).

In Iceland, rivers draining older catchments ($>10^6$ years) are undersaturated with respect to these high ^{187}Re/^{188}Os bearing minerals (olivine, pyroxene, and plagioclase) and preferential weathering of these phases from the host basalt, combined with their age, which allows for radiogenic ingrowth of ^{187}Os from the decay of ^{187}Re, causes elevated radiogenic ^{187}Os/^{188}Os in the dissolved load (^{187}Os/^{188}Os = 0.55, ^{187}Re/^{188}Os = 752; Table S4; Gannoun et al., 2006). In contrast, rivers draining younger catchments ($<10^6$ years) are approaching saturation with respect to these same minerals, which in this instance have not had time to attain significant radiogenic ingrowth of ^{187}Os, and weathering tends toward congruency causing the dissolved load to approach that of bulk-rock (^{187}Os/^{188}Os = 0.2, ^{187}Re/^{188}Os = 196; Table S4; Gannoun et al., 2006).

When the ^{187}Os/^{188}Os of macroalgae is shown against the reciprocal of the concentration, while utilizing the ^{187}Re/^{188}Os of macroalgae (color code in Figure 7) as an indication of marine over freshwater influence (see Figure 6b), the ^{187}Os/^{188}Os for macroalgae fall within a field delimited by three potential end-members (Figure 7a): seawater (radiogenic ^{187}Os/^{188}Os, intermediate [Os], and high ^{187}Re/^{188}Os), river water draining an old basaltic catchment (less radiogenic ^{187}Os/^{188}Os, low [Os], and intermediate ^{187}Re/^{188}Os), and geothermal water and river water draining a young basaltic catchment (unradiogenic ^{187}Os/^{188}Os, high [Os], and low ^{187}Re/^{188}Os).

Racionero-Gómez et al. (2017) cultured *F. vesiculosus* in seawater of varying Os concentrations with a known ^{187}Os/^{188}Os composition (~0.16). This study found that as the Os concentration of the seawater culture medium increased, the Os abundance in macroalgae increased following the relationship: [Os]$_{seawater}$ = 0.0004 · [Os]$_{F. vesiculosus}$$^{1.6607}$ (R^2 = 0.99, *p*-value =- 0.005). We can utilize this relationship to convert the Os abundance of Icelandic *F. vesiculosus* measured in this study, into the average Os abundance of the seawater in which that macroalgae lived. When the reciprocal of this value is plotted against the ^{187}Os/^{188}Os of *F. vesiculosus* (Figure 7b), the data fall within a field delimited by three end-members similar to Figure 7a. When compared to an idealized three-point end-member mixing model for Icelandic waters (Figure 7b), data fall upon either: a mixing line between seawater (light grey end-member in Figure 7b; ^{187}Os/^{188}Os = 1.02, [Os] = 10 ppq, and ^{187}Re/^{188}Os = 4198) and direct-runoff rivers draining old catchments (dark grey end-member in Figure 7b; ^{187}Os/^{188}Os = 0.6, [Os] = 3.5 ppq, and ^{187}Re/^{188}Os = 191 to 1659); a mixing line between seawater and direct-runoff rivers draining young rivers or geothermal waters (black end-member in Figure 7b; ^{187}Os/^{188}Os = 0.14, [Os] = 22.7 ppq, and ^{187}Re/^{188}Os = 122 to 338); or, close to the value for seawater itself (Figure 7b; Table S4; Colodner et al., 1993b; Gannoun et al., 2006; Gannoun & Burton, 2014). However, the data are offset in concentration space from an idealized mixing model. This is most likely caused by the conversion factor used, which was developed by doping macroalgae under exceptionally high seawater Os concentrations (Racionero-Gómez et al., 2017).

The ^{187}Re/^{188}Os of *F. vesiculosus* (contours in Figure 7b) maintains a similar relationship to Figure 7a, with high ^{187}Re/^{188}Os clustered around the seawater end-member. However, one sample has a ^{187}Re/^{188}Os value (~39,000) indicative of seawater despite a 1/[Os] (~128) and ^{187}Os/^{188}Os (~0.75) indicative of river water draining an old basaltic catchment (Figure 7b). This is due to the weathering of basaltic minerals with relatively radiogenic ^{187}Os/^{188}Os (0.13 to 0.25, which has undergone radiogenic ingrowth) and high ^{187}Re/^{188}Os (288 to 7164) ratios (Burton et al., 2002; Gannoun et al., 2004, 2006), driving the ^{187}Re/^{188}Os

of macroalgae near older river catchments to ratios comparable to more marine habitats. Macroalgae therefore hold the potential to not only record the $^{187}Os/^{188}Os$ of the water in which they live but also be qualitatively used to determine the relative $^{187}Re/^{188}Os$ ratio of the water in which they live (See Figures 5d, 6b, and 7).

5. Conclusions

The Re-Os data for macroalgae presented here have been successfully used to trace the influence of basaltic weathering on the Re and Os isotope systematics of Icelandic coastal waters and show the influence of seawater in an estuarine setting, providing further evidence to support the use of the $^{187}Os/^{188}Os$ of macroalgae as a proxy for the $^{187}Os/^{188}Os$ of seawater. As such, the latter presents a more amenable option to direct seawater analysis, potentially becoming a useful tool for tracing a variety of Earth system processes. Additionally, in keeping with previous work, we have shown that Re and Os is taken up by macroalgae from the dissolved load of the seawater it inhabits. However, unlike previous work, we also suggest that additional uptake of both Re and Os could occur from the bed load. However, experimental studies similar to those done for Re and Os uptake from dissolved load (Racionero-Gómez et al., 2016; Racionero-Gómez et al., 2017) are needed for both bed and suspended particulate load to assess the influence of these phases on the Re-Os systematics of macroalgae.

Looking to the future, if the macroalgae obtained in this study at the mouth of a river represents the entire drainage area (Miller et al., 2011), then the entire quantity and isotopic composition of dissolved Os that is supplied to the North Atlantic from Icelandic rivers can be estimated. The rivers in proximity to *F. vesiculosus* studied here have an annual discharge of 2.3 km^3/year, accounting for 1.3% of the total discharge of Icelandic rivers (175 km^3/year). Given the Os abundance of *F. vesiculosus*, which has been converted to that of seawater and then offset to be more representative of Icelandic geochemical reservoirs (see Figure 7b), we estimate a dissolved Os flux of 2.35 kg/year. These values are far higher than previously recorded estimates for Icelandic rivers of 0.98 kg/year (Gannoun et al., 2006). Some of the discrepancy between these two values is likely due to the underrepresentation of Icelandic rivers in this study (1.3%) when compared to previous studies (21%; Gannoun et al., 2006) and the potential additional uptake of Os from the underlying bed load but may also suggest that more work is needed to understand the uptake rate of Os by macroalgae at natural levels in order to determine an accurate estimate for the abundance of Os in seawater. As such, experimental studies conducted at natural Os levels to determine the Os uptake rate of common macroalgae species combined with Al and/or Fe analysis of field samples to remove potential bed load contamination could allow macroalgae to be utilized to estimate the global riverine abundance and flux of Os to the ocean, yielding a better understanding of the global Os cycle and oceanic residence times.

References

Anbar, A. D., Creaser, R. A., Papanastassiou, D. A., & Wasserburg, G. J. (1992). Rhenium in seawater: Confirmation of generally conservative behavior. *Geochimica et Cosmochimica Acta*, *56*(11), 4099–4103. Retrieved from http://www.sciencedirect.com/science/article/pii/001670379290021A, https://doi.org/10.1016/0016-7037(92)90021-A

Barreiro, R., Picado, L., & Real, C. (2002). Biomonitoring heavy metals in estuaries: A field comparison of two brown algae species inhabiting upper estuarine reaches. *Environmental Monitoring and Assessment*, *75*(2), 121–134. https://doi.org/10.1023/A:1014479612811

Birck, J. L., Barman, M. R., & Capmas, F. (1997). Re-Os isotopic measurements at the femtomole level in natural samples. *Geostandards Newsletter*, *21*(1), 19–27. https://doi.org/10.1111/j.1751-908X.1997.tb00528.x

Bryan, G., & Hummerstone, L. (1973). Brown seaweed as an indicator of heavy metals in estuaries in south-west England. *Journal of the Marine Biological Association of the United Kingdom*, *53*(03), 705–720. https://doi.org/10.1017/S0025315400058902

Burdon-Jones, C., Denton, G., Jones, G. B., & McPhie, K. (1982). Regional and seasonal variations of trace metals in tropical Phaeophyceae from North Queensland. *Marine Environmental Research*, *7*(1), 13–30. https://doi.org/10.1016/0141-1136(82)90048-4

Burton, K. W., Gannoun, A., Birck, J.-L., Allègre, C. J., Schiano, P., Clocchiatti, R., & Alard, O. (2002). The compatibility of rhenium and osmium in natural olivine and their behaviour during mantle melting and basalt genesis. *Earth and Planetary Science Letters*, *198*(1-2), 63–76. https://doi.org/10.1016/S0012-821X(02)00518-6

Carlson, L. (1991). Seasonal variation in growth, reproduction and nitrogen content of Fucus vesiculosus L. in the Öresund, Southern Sweden. *Botanica Marina*, *34*(5), 447–454.

Chen, C., Sedwick, P. N., & Sharma, M. (2009). Anthropogenic osmium in rain and snow reveals global-scale atmospheric contamination. *Proceedings of the National Academy of Sciences*, *106*(19), 7724–7728. Retrieved from http://www.pnas.org/content/106/19/7724.abstract, https://doi.org/10.1073/pnas.0811803106

Chen, C., & Sharma, M. (2009). High precision and high sensitivity measurements of osmium in seawater. *Analytical Chemistry*, *81*(13), 5400–5406. https://doi.org/10.1021/ac900600e

Cohen, A. S., & Waters, F. G. (1996). Separation of osmium from geological materials by solvent extraction for analysis by thermal ionisation mass spectrometry. *Analytica Chimica Acta*, *332*(2-3), 269–275. https://doi.org/10.1016/0003-2670(96)00226-7

Colodner, D., Edmond, J., & Boyle, E. (1995). Rhenium in the Black Sea: Comparison with molybdenum and uranium. *Earth and Planetary Science Letters*, *131*(1-2), 1–15. Retrieved from http://www.sciencedirect.com/science/article/pii/0012821X9500010A, https://doi.org/10.1016/0012-821X(95)00010-A

Colodner, D., Sachs, J., Ravizza, G., Turekian, K., Edmond, J., & Boyle, E. (1993a). The geochemical cycle of rhenium: A reconnaissance. *Earth and Planetary Science Letters*, *117*(1–2), 205–221. https://doi.org/10.1016/0012-821X(93)90127-U

Colodner, D. C., Boyle, E. A., & Edmond, J. M. (1993b). Determination of rhenium and platinum in natural waters and sediments, and iridium in sediments by flow injection isotope dilution inductively coupled plasma mass spectrometry. *Analytical Chemistry*, *65*(10), 1419–1425. https://doi.org/10.1021/ac00058a019

Connan, S., & Stengel, D. B. (2011). Impacts of ambient salinity and copper on brown algae: 1. Interactive effects on photosynthesis, growth, and copper accumulation. *Aquatic Toxicology*, *104*(1-2), 94–107. Retrieved from http://www.sciencedirect.com/science/article/pii/S0166445X11000944, https://doi.org/10.1016/j.aquatox.2011.03.015

Creaser, R. A., Papanastassiou, D. A., & Wasserburg, G. J. (1991). Negative thermal ion mass spectrometry of osmium, rhenium and iridium. *Geochimica et Cosmochimica Acta*, *55*(1), 397–401. Retrieved from http://www.sciencedirect.com/science/article/pii/0016703791904277, https://doi.org/10.1016/0016-7037(91)90427-7

Cumming, V. M., Poulton, S. W., Rooney, A. D., & Selby, D. (2013). Anoxia in the terrestrial environment during the late Mesoproterozoic. *Geology*, *41*(5), 583–586. https://doi.org/10.1130/G34299.1

Debaille, V., Trønnes, R. G., Brandon, A. D., Waight, T. E., Graham, D. W., & Lee, C.-T. A. (2009). Primitive off-rift basalts from Iceland and Jan Mayen: Os-isotopic evidence for a mantle source containing enriched subcontinental lithosphere. *Geochimica et Cosmochimica Acta*, *73*(11), 3423–3449. https://doi.org/10.1016/j.gca.2009.03.002

Fuge, R., & James, K. (1973). Trace metal concentrations in brown seaweeds, Cardigan Bay, Wales. *Marine Chemistry*, *1*(4), 281–293. https://doi.org/10.1016/0304-4203(73)90018-2

Gannoun, A., & Burton, K. W. (2014). High precision osmium elemental and isotope measurements of North Atlantic seawater. *Journal of Analytical Atomic Spectrometry*, *29*(12), 2330–2342. https://doi.org/10.1039/C4JA00265B

Gannoun, A., Burton, K. W., Thomas, L. E., Parkinson, I. J., van Calsteren, P., & Schiano, P. (2004). Osmium isotope heterogeneity in the constituent phases of mid-ocean ridge basalts. *Science*, *303*(5654), 70–72. https://doi.org/10.1126/science.1090266

Gannoun, A., Burton, K. W., Vigier, N., Gíslason, S. R., Rogers, N., Mokadem, F., & Sigfússon, B. (2006). The influence of weathering process on riverine osmium isotopes in a basaltic terrain. *Earth and Planetary Science Letters*, *243*(3–4), 732–748. https://doi.org/10.1016/j.epsl.2006.01.024

Gunnarsson, K., & Ingolfsson, A. (1995). Seasonal changes in the abundance of intertidal algae in Southwestern Iceland. *Botanica Marina*, *38*(1–6), 69–78.

Haritonidis, S., & Malea, P. (1999). Bioaccumulation of metals by the green alga Ulva rigida from Thermaikos Gulf, Greece. *Environmental Pollution*, *104*(3), 365–372. Retrieved from http://www.sciencedirect.com/science/article/pii/S0269749198001924, https://doi.org/10.1016/S0269-7491(98)00192-4

Ho, Y. B. (1990). Ulva lactuca as bioindicator of metal contamination in intertidal waters in Hong Kong. *Hydrobiologia*, *203*(1-2), 73–81. https://doi.org/10.1007/BF00005615

Horan, K., Hilton, R. G., Selby, D., Ottley, C. J., Gröcke, D. R., Hicks, M., & Burton, K. W. (2017). Mountain glaciation drives rapid oxidation of rock-bound organic carbon. *Science Advances*, *3*(10). https://doi.org/10.1126/sciadv.1701107, http://advances.sciencemag.org/content/3/10/e1701107.abstract

Ishikawa, A., Senda, R., Suzuki, K., Dale, C. W., & Meisel, T. (2014). Re-evaluating digestion methods for highly siderophile element and [187]Os isotope analysis: Evidence from geological reference materials. *Chemical Geology*, *384*, 27–46. https://doi.org/10.1016/j.chemgeo.2014.06.013

Jóhannesson, H. (2014). Geological Map of Iceland. 1:600 000. Bedrock Geology. *Icelandic Institute of Natural History, Reykjavik (2nd edition)*.

Levasseur, S., Birck, J.-L., & Allegre, C. (1999). The osmium riverine flux and the oceanic mass balance of osmium. *Earth and Planetary Science Letters*, *174*(1-2), 7–23. https://doi.org/10.1016/S0012-821X(99)00259-9

Levasseur, S., Birck, J.-L., & Allègre, C. J. (1998). Direct measurement of femtomoles of osmium and the [187]Os/[186]Os ratio in seawater. *Science*, *282*(5387), 272–274. https://doi.org/10.1126/science.282.5387.272

Levasseur, S., Rachold, V., Birck, J.-L., & Allegre, C. (2000). Osmium behavior in estuaries: The Lena River example. *Earth and Planetary Science Letters*, *177*(3-4), 227–235. https://doi.org/10.1016/S0012-821X(00)00049-2

Luoma, S. N., Bryan, G. W., & Langston, W. J. (1982). Scavenging of heavy metals from particulates by brown seaweed. *Marine Pollution Bulletin*, *13*(11), 394–396. Retrieved from http://www.sciencedirect.com/science/article/pii/0025326X82901163, https://doi.org/10.1016/0025-326X(82)90116-3

Malea, P., Haritonidis, S., & Kevrekidis, T. (1995). Metal content of some green and brown seaweeds from Antikyra Gulf (Greece). *Hydrobiologia*, *310*(1), 19–31. https://doi.org/10.1007/BF00008180

Martin, C. E., Peucker-Ehrenbrink, B., Brunskill, G., & Szymczak, R. (2001). Osmium isotope geochemistry of a tropical estuary. *Geochimica et Cosmochimica Acta*, *65*(19), 3193–3200. https://doi.org/10.1016/S0016-7037(01)00654-8

Mas, J., Tagami, K., & Uchida, S. (2005). Rhenium measurements on North Atlantic seaweed samples by ID-ICP-MS: An observation on the Re concentration factors. *Journal of Radioanalytical and Nuclear Chemistry*, *265*(3), 361–365. https://doi.org/10.1007/s10967-005-0833-3

Mathieson, A. C., Shipman, J. W., O'shea, J. R., & Hasevlat, R. C. (1976). Seasonal growth and reproduction of estuarine fucoid algae in New England. *Journal of Experimental Marine Biology and Ecology*, *25*(3), 273–284. https://doi.org/10.1016/0022-0981(76)90129-5

Melián, C., Kremer, C., Suescun, L., Mombrú, A., Mariezcurrena, R., & Kremer, E. (2000). Re (V) complexes with amino acids based on the '3+2' approach. *Inorganica Chimica Acta*, *306*(1), 70–77. Retrieved from http://www.sciencedirect.com/science/article/pii/S0020169300001511, https://doi.org/10.1016/S0020-1693(00)00151-1

Miller, C. A., Peucker-Ehrenbrink, B., Walker, B. D., & Marcantonio, F. (2011). Re-assessing the surface cycling of molybdenum and rhenium. *Geochimica et Cosmochimica Acta*, *75*(22), 7146–7179. https://doi.org/10.1016/j.gca.2011.09.005

Munda, I. (1972). On the chemical composition, distribution and ecology of some common benthic marine algae from Iceland. *Botanica Marina*, *15*, 1.

Munda, I. (1975). Hydrographically conditioned floristic and vegetation limits in Icelandic coastal waters. *Botanica Marina*, *18*, 223.

Munda, I. M. (1987). Distribution and use of some economically important seaweeds in Iceland. *Hydrobiologia*, *151*(1), 257–260.

Niemeck, R. A., & Mathieson, A. C. (1976). An ecological study of Fucus spiralis L. *Journal of Experimental Marine Biology and Ecology*, *24*(1), 33–48. https://doi.org/10.1016/0022-0981(76)90041-9

Nowell, G., Luguet, A., Pearson, D., & Horstwood, M. (2008). Precise and accurate 186 Os/188 Os and ^{187}Os/^{188}Os measurements by multi-collector plasma ionisation mass spectrometry (MC-ICP-MS) part I: Solution analyses. *Chemical Geology*, *248*(3-4), 363–393. https://doi.org/10.1016/j.chemgeo.2007.10.020

Paul, M., Reisberg, L., & Vigier, N. (2009). A new method for analysis of osmium isotopes and concentrations in surface and subsurface water samples. *Chemical Geology*, *258*(3-4), 136–144. https://doi.org/10.1016/j.chemgeo.2008.09.018

Peckol, P., Harlin, M. M., & Krumscheid, P. (1988). Physiological and population ecology of intertidal and subtidal Ascophyllum nodosum (Phaeophyta). *Journal of Phycology*, *24*(2), 192–198. https://doi.org/10.1111/j.1529-8817.1988.tb00077.x

Peucker-Ehrenbrink, B., & Ravizza, G. (2000). The marine osmium isotope record. *Terra Nova*, *12*(5), 205–219. https://doi.org/10.1046/j.1365-3121.2000.00295.x

Peucker-Ehrenbrink, B., & Ravizza, G. (2012). Chapter 8—Osmium isotope stratigraphy. In *The geologic time scale* (pp. 145–166). Boston: Elsevier.

Peucker-Ehrenbrink, B., Sharma, M., & Reisberg, L. (2013). Recommendations for analysis of dissolved osmium in seawater. *Eos, Transactions American Geophysical Union*, *94*(7), 73–73. https://doi.org/10.1002/2013EO070006

Prouty, N. G., Roark, E. B., Koenig, A. E., Demopoulos, A. W., Batista, F. C., Kocar, B. D., et al. (2014). Deep-sea coral record of human impact on watershed quality in the Mississippi River Basin. *Global Biogeochemical Cycles*, *28*, 29–43. https://doi.org/10.1002/2013GB004754

Racionero-Gómez, B., Sproson, A., Selby, D., Gröcke, D., Redden, H., & Greenwell, H. (2016). Rhenium uptake and distribution in phaeophyceae macroalgae, Fucus vesiculosus. *Royal Society Open Science*, *3*(5), 160161. https://doi.org/10.1098/rsos.160161

Racionero-Gómez, B., Sproson, A. D., Selby, D., Gannoun, A., Gröcke, D. R., Greenwell, H. C., & Burton, K. W. (2017). Osmium uptake, distribution, and ^{187}Os/^{188}Os and ^{187}Re/^{188}Os compositions in *Phaeophyceae macroalgae*, *Fucus vesiculosus*: Implications for determining the ^{187}Os/^{188}Os composition of seawater. *Geochimica et Cosmochimica Acta*, *199*, 48–57. https://doi.org/10.1016/j.gca.2016.11.033

Ragan, M. A., Smidsrød, O., & Larsen, B. (1979). Chelation of divalent metal ions by brown algal polyphenols. *Marine Chemistry*, *7*(3), 265–271. Retrieved from http://www.sciencedirect.com/science/article/pii/0304420379900434, https://doi.org/10.1016/0304-4203(79)90043-4

Rainbow, P. S. (1995). Biomonitoring of heavy metal availability in the marine environment. *Marine Pollution Bulletin*, *31*(4-12), 183–192. Retrieved from http://www.sciencedirect.com/science/article/pii/0025326X95001165, https://doi.org/10.1016/0025-326X(95)00116-5

Rice, D. L., & Lapointe, B. E. (1981). Experimental outdoor studies with Ulva fasciata Delile. II. Trace metal chemistry. *Journal of Experimental Marine Biology and Ecology*, *54*(1), 1–11. https://doi.org/10.1016/0022-0981(81)90098-8

Rönnberg, O., Adjers, K., Ruokolahti, C., & Bondestam, M. (1990). Fucus vesiculosus as an indicator of heavy metal availability in a fish farm recipient in the northern Baltic Sea. *Marine Pollution Bulletin*, *21*(8), 388–392. Retrieved from http://www.sciencedirect.com/science/article/pii/0025326X9090648R, https://doi.org/10.1016/0025-326X(90)90648-R

Rooney, A. D., Selby, D., Lloyd, J. M., Roberts, D. H., Lückge, A., Sageman, B. B., & Prouty, N. G. (2016). Tracking millennial-scale Holocene glacial advance and retreat using osmium isotopes: Insights from the Greenland ice sheet. *Quaternary Science Reviews*, *138*, 49–61. https://doi.org/10.1016/j.quascirev.2016.02.021

Scadden, E. M. (1969). Rhenium: Its concentration in Pacific Ocean surface waters. *Geochimica et Cosmochimica Acta*, *33*(5), 633–637. Retrieved from http://www.sciencedirect.com/science/article/pii/0016703769900192, https://doi.org/10.1016/0016-7037(69)90019-2

Sharma, M., Balakrishna, K., Hofmann, A. W., & Shankar, R. (2007). The transport of osmium and strontium isotopes through a tropical estuary. *Geochimica et Cosmochimica Acta*, *71*(20), 4856–4867. https://doi.org/10.1016/j.gca.2007.08.004

Sharma, M., Chen, C., & Blazina, T. (2012). Osmium contamination of seawater samples stored in polyethylene bottles. *Limnology and Oceanography: Methods*, *10*(9), 618–630.

Sharma, M., Papanastassiou, D., & Wasserburg, G. (1997). The concentration and isotopic composition of osmium in the oceans. *Geochimica et Cosmochimica Acta*, *61*(16), 3287–3299. https://doi.org/10.1016/S0016-7037(97)00210-X

Sharma, M., & Wasserburg, G. (1997). Osmium in the rivers. *Geochimica et Cosmochimica Acta*, *61*(24), 5411–5416. https://doi.org/10.1016/S0016-7037(97)00329-3

Sideman, E. J., & Mathieson, A. C. (1983). Ecological and genecological distinctions of a high intertidal dwarf form of Fucus distichus (L.) Powell in New England. *Journal of Experimental Marine Biology and Ecology*, *72*(2), 171–188. https://doi.org/10.1016/0022-0981(83)90142-9

Strömgren, T. (1977). Short-term effects of temperature upon the growth of intertidal Fucales. *Journal of Experimental Marine Biology and Ecology*, *29*(2), 181–195. https://doi.org/10.1016/0022-0981(77)90047-8

Turekian, K. K., Sharma, M., & Gordon, G. W. (2007). The behavior of natural and anthropogenic osmium in the Hudson River–Long Island Sound estuarine system. *Geochimica et Cosmochimica Acta*, *71*(17), 4135–4140. https://doi.org/10.1016/j.gca.2007.05.020

Viana, I. G., Aboal, J. R., Fernández, J. A., Real, C., Villares, R., & Carballeira, A. (2010). Use of macroalgae stored in an environmental specimen bank for application of some European Framework Directives. *Water Research*, *44*(6), 1713–1724. Retrieved from http://www.sciencedirect.com/science/article/pii/S0043135409007817, https://doi.org/10.1016/j.watres.2009.11.036

Völkening, J., Walczyk, T., & Heumann, K. G. (1991). Osmium isotope ratio determinations by negative thermal ionization mass spectrometry. *International Journal of Mass Spectrometry and Ion Processes*, *105*(2), 147–159. https://doi.org/10.1016/0168-1176(91)80077-Z

Woodhouse, O., Ravizza, G., Falkner, K. K., Statham, P., & Peucker-Ehrenbrink, B. (1999). Osmium in seawater: Vertical profiles of concentration and isotopic composition in the eastern Pacific Ocean. *Earth and Planetary Science Letters*, *173*(3), 223–233. https://doi.org/10.1016/S0012-821X(99)00233-2

Xiong, Y., Xu, J., Shan, W., Lou, Z., Fang, D., Zang, S., & Han, G. (2013). A new approach for rhenium (VII) recovery by using modified brown algae Laminaria japonica adsorbent. *Bioresource Technology*, *127*, 464–472. Retrieved from http://www.sciencedirect.com/science/article/pii/S0960852412014496, https://doi.org/10.1016/j.biortech.2012.09.099

Yang, J. S. (1991). High rhenium enrichment in brown algae: A biological sink of rhenium in the sea? *Hydrobiologia*, *211*(3), 165–170. https://doi.org/10.1007/BF00008532

Yeghicheyan, D., Bossy, C., Bouhnik Le Coz, M., Douchet, C., Granier, G., Heimburger, A., et al. (2013). A compilation of silicon, rare Earth element and twenty-one other trace element concentrations in the natural river water reference material SLRS-5 (NRC-CNRC). *Geostandards and Geoanalytical Research*, *37*(4), 449–467. https://doi.org/10.1111/j.1751-908X.2013.00232.x